Jestr

Journal of Engineering Science and Technology Review 17 (4) (2024) 128-135

Research Article

JOURNAL OF
Engineering Science and Technology Review

www.jestr.org

Design and Simulation of a Millimeter and Submillimeter Detector Utilizing a High-Temperature Superconductor Josephson Junction

Zahra Ehsani, Mahboobeh Baghi Hedeshi and Seyed Mohammad Hassan Javadzadeh*

Department of Electrical Engineering, Shahed University, Tehran, Iran

Received 25 April 2024; Accepted 7 June 2024

Abstract

Superconducting detectors play a crucial role in astronomy, particularly at millimeter and sub-millimeter wavelengths, due to their high sensitivity, ease of fabrication, and potential for integration into large arrays. Josephson junction detectors, which utilize high-temperature superconductors, offer a promising design option because they can operate at higher temperatures. In this paper, we aim to design and simulate two detectors based on high-temperature Josephson junctions for millimeter and sub-millimeter waves. To achieve this goal, we employed the Riblet directional coupler to develop detector arrays. We evaluated the frequency response, quality factor, and loss in these detectors. The experimental results indicate that constructing larger arrays and reducing the gap between the coupler and resonators can enhance the quality factor. We demonstrate this improvement by presenting the quality factors for two different gaps in each spectrum.

Keywords: Superconductor, Josephson Junction, Hybrid microstrip resonator, Submillimeter wave, Riblet type directional coupler.

1. Introduction

Millimeter and submillimeter waves, covering a frequency range of approximately 30 GHz to 3 THz, constitute one of the most significant yet underdeveloped parts of the electromagnetic spectrum [1]. Observations within this spectrum are crucial for understanding the universe, given that Earth's atmosphere is partially transmissive at these wavelengths [2]. Additionally, this range includes a substantial amount of Cosmic Microwave Background (CMB) energy, which is invaluable for studying the early universe [1]. One of the advantages of radiation in this spectrum is the shorter wavelength, allowing for reduced component size in instruments—an ideal feature for various applications, including missiles, satellites, and aircraft. The short wavelength also results in narrower bandwidth, leading to improved resolution and precision [3]. Moreover, imaging devices operating in these wavelengths can be effectively used in adverse visibility conditions, such as fog and night [4]. Given the significance of observations in the sub-mm/far-IR range, there is a pressing need for the development of novel and more sensitive detectors for large-scale arrays. To achieve high sensitivity, low-temperature detectors are required, making superconductors the ideal materials due to their potential for providing the necessary sensitivity for astronomical observations [5]. Various superconducting detectors have been designed for operating in this range, including Hot electron bolometers (HEBs), spin-torque microwave detectors, superconducting single-photon detectors, microwave kinetic inductance detectors (MKIDs), and detectors based on superconducting tunnel junctions, also known as Josephson junctions [6]. A superconducting tunnel junction (STJ) consists of two superconductors separated by a thin insulator. In simple terms, tunnel junctions can filter out the Cooper pairs while allowing the quasi-particles to pass. Photons can break apart a large number of Cooper pairs, generating quasi-particles and resulting in a current pulse flowing through the junction. The amplitude of this current indicates the energy of the event. Consequently, when a superconductor absorbs a steady flux of submm photons, a dc current is produced in the junction. This phenomenon makes SIS junctions promising candidates for highly sensitive detectors in the submm/far-IR spectrum [7]. Detectors based on the tunnelling of quasiparticles in superconducting tunnel junctions can, in some cases, be built into systems with sensitivity near the fundamental limit, making them very desirable [8]. Moreover, they exhibit extremely low noise levels, as low as 10^{-19} [1]. In the current research, our purpose is to design and simulate two detectors based on high-temperature Josephson junctions for millimeter and sub-millimeter waves as follows:

- We designed a Cu strip resonator detector for the millimeter wave spectrum.
- We built this detector in arrays of two, four, and six detectors using a Riblet short-slot coupler.
- We measured the quality factor and loss with the gap between the coupler and the resonator at 0.1 mm and 0.5 mm.
- We designed a YCBO strip resonator detector for the sub-millimeter spectrum and built it into arrays of two, four, and six resonators using an adjusted Riblet short-slot coupler.
- Similarly, we calculated the quality factor and loss with the gap between the coupler and the resonator at 0.1 mm and 0.001 mm.

2. Tunneling in Superconductors and Josephson Effect

*E-mail address: mbaghihedeshi@gmail.com
ISSN: 1791-2377
doi:10.25103/jestr.174.15

Quantum mechanics dictates that particles, such as electrons, possess a finite probability of penetrating forbidden areas. Consequently, they can tunnel through potential barriers that separate two permissible regions. The probability of tunneling exponentially depends on the barrier's width, making it feasible only for small barriers [9]. Superconductors exhibit various configurations that allow the tunneling phenomenon: Superconductor Insulator Normal (SIN), which occurs when an insulator barrier is placed between a bulk of superconductor and normal metal [10], Superconductor Insulator Superconductor (SIS), also known as Josephson junction, involving two superconductors and an insulator barrier [11], Superconductor Normal Superconductor (SNS) [12], Superconductor Ferromagnetic Superconductor (SFS); and Superconductor Insulator Ferromagnetic Superconductor (SIFS) [11].

In 1962, B.D. Josephson investigated two superconductors separated by an insulating barrier, a structure later termed the Josephson Junction. The insulating barrier must be thin to allow electron tunneling. Figure 1 displays the wave function for electrons on each bulk of superconductor. When no voltage is applied to the junction, the chemical potential remains constant on either side, resulting in a constant phase difference and a steady supercurrent flowing through the junction. This phenomenon is known as the DC Josephson effect, where the macroscopic phase difference between the superconductors determines the supercurrent through the junction [13]. Applying a DC voltage (V) to the junction leads to an AC current flowing through it at a frequency of $^{2eV}/_{\hbar}$. This phenomenon is referred to as the AC Josephson effect.

$$I(t) = I_C \sin(^{2eV}/_{\hbar}) \quad (1)$$

I_c in Equation (1) indicates critical current, where $K_j = {}^{2e}/_{\hbar} = 483\,597.9\,GHz/V$ is known as the Josephson constant. In Figure 2 illustrates the voltage-current characteristics of a Josephson Junction.

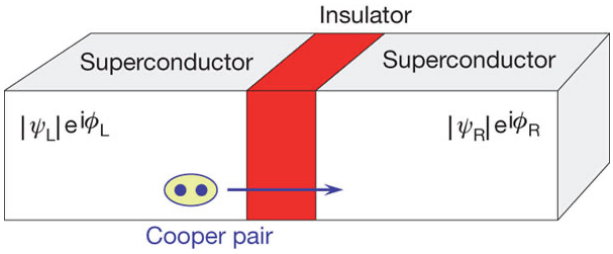

Fig. 1. Schematic of a Josephson Junction and the tunneling of cooper pairs

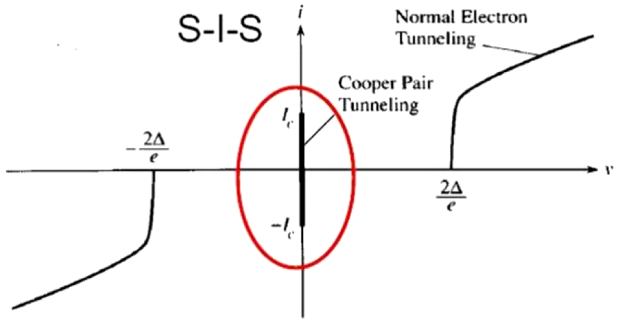

Fig. 2. voltage-current characteristics of a Josephson Junction.

Josephson junctions can be categorized into two types based on their junction length: short Josephson junctions (SJJ) and long Josephson junctions (LJJ). A short Josephson junction (SJJ) is one where the junction width is smaller than the Josephson penetration depth. Conversely, a long Josephson junction (LJJ) is defined by a width that exceeds the Josephson penetration depth [14]. For SJJs, the supercurrent density can be considered uniform and close to the critical current density. However, in LJJs, the supercurrent is less uniform, exhibiting two peaks in the distribution [15]. In short junctions, the magnetic field created by the Josephson current itself, also known as the self-field, is much smaller than the externally applied magnetic field. However, this is no longer the case for long junctions. When Josephson junctions display a spatially homogeneous supercurrent density and phase difference, they are referred to as lumped junctions [10].

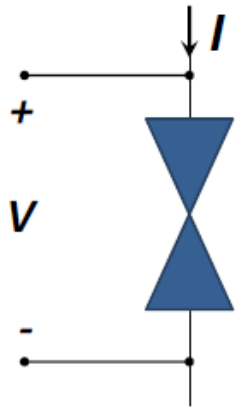

Fig. 3. A Josephson junction depicted as a lumped circuit element [10].

The energy stored in the junction can be determined using Equation 2 [10].

$$E_J = \frac{\Phi_0 I_C}{2\pi}(1 - \cos\varphi) \quad (2)$$

In this equation $\Phi_0 = {}^{\hbar}/_{2e}$, and φ represents the phase difference.

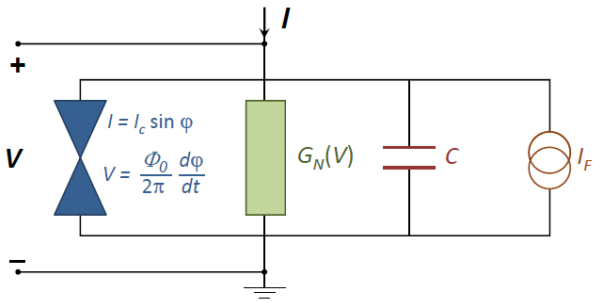

Fig. 4. A Josephson junction equivalent circuit

Figure 4 illustrates the equivalent circuit for a Josephson junction. $G_N(V)$ denotes the normal conductance of the junction, C is the junction capacitance, and I_F represents the noise fluctuations. At T=0, for a junction with a natural resistance of R_N, area of A_i, thickness of d and dielectric constant of ε we can calculate $G_N(V)$ and C using equations 3 and 4 [10].

$$G_N(V) = \begin{cases} 0, & |V| < 2\Delta/e \\ \frac{1}{R_N}, & |V| \geq 2\Delta/e \end{cases} \quad (3)$$

$$C = \frac{\varepsilon\varepsilon_0 A_i}{d} \quad (4)$$

3. High Temperature Josephson Junction Detectors

The structure of high-temperature superconductors (HTS) and low-temperature superconductors (LTS) differs significantly. Among the most extensively studied compounds is $YBa_2Cu_3O_{7-x}$ also known as YBCO [16]. YBCO exhibits an energy gap ranging from 10 to 60 meV and possesses a critical temperature of over 80 K, making it a promising candidate for HTS THz detectors. HTS devices operate at higher temperatures, thereby reducing cryogenic costs. Additionally, they can achieve response frequencies well into the THz range, thanks to their higher energy gap compared to LTS devices [17]. As discussed in the previous section, the AC Josephson effect demonstrates that when the current exceeds the junction critical current, a DC voltage (V_0) emerges across the junction. Consequently, the phase difference varies with time, following the voltage-frequency relationship $f = {2eV_0}/{\hbar}$. When an RF wave is applied to the junction:

$$V(t) = V_0 + V_m \cos \omega \tag{5}$$

As a result, the junction current can be calculated using equation 6:

$$I(t) = I_c \sum J_n(4\pi eV_m/\hbar\omega) \sin\left[(\omega_j + n\omega)t + \theta_0\right] \tag{6}$$

Here $J_n(x)$ represents the nth order Bessel junction. Consequently, the DC voltage and current can be determined.

$$V_0 = n({\hbar f}/{2e}) \tag{7}$$

$$I_0 = (-1)^n I_C J_n({2eV_m}/{\hbar f}) \sin\theta_0 \tag{8}$$

This analysis demonstrates that when an RF signal is applied to the Josephson junction, it generates a series of steps with a voltage separation of ${\hbar f}/{2e}$. These steps are observable in the DC I-V curve and are referred to as Shapiro steps. This behavior forms the basis for RF detection in Josephson junctions. Figure 5 serves as an illustrative example, depicting Shapiro steps in the I-V curves of a ring-slot antenna-coupled HTS step-edge junction. Clearly, from this figure, we can observe that as RF power increases, the current step-height also increases, while the junction critical current decreases [18].

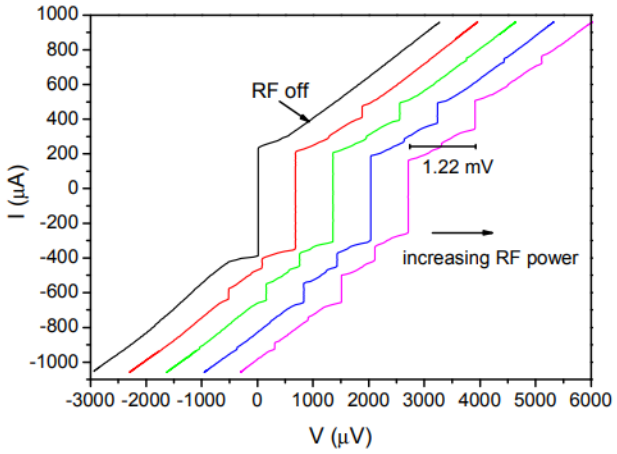

Fig. 5. An example of Shapiro steps in a I-V curve [18].

Quasiclassical high-temperature Josephson detectors can operate at temperatures as high as 50K and provide a bandwidth of up to 1 THz, with noise levels as low as 10^{-14} $W/\sqrt{Hz}$ [19]. These detectors are suitable for terahertz imaging in medical and security screening applications [20].

A high-sensitivity rounded bow-tie antenna, coupled with a bicrystal Josephson junction detector containing a thin layer of YBCO, is precisely positioned at the bicrystal misorientation point in the antenna's center for detecting THz waves. These devices operate at 60 K, offering a voltage sensitivity of 30 dB and a noise equivalent power of 10^{-12} $W/\sqrt{Hz}$ [21]. The sensitivity of this configuration can be further enhanced by using a serial antenna array of Josephson junctions, increasing the effective detection area and resulting in an improvement in the total equivalent RF power detected [22].

Graphene-based Josephson junction bolometers embedded in microwave resonators demonstrate over 99% coupling efficiency, high resolution, and a noise equivalent power of around 10^{-19} $W/\sqrt{Hz}$. These devices outperform HEBs in terms of speed and do not rely on breaking Cooper pairs to generate a detectable signal, making them an appealing choice for continuous photon sensing applications [23].

Among the challenging Josephson-based detectors are Josephson junction single-photon detectors, which require deliberate suppression of Josephson coupling using an external magnetic field to be sensitive enough to detect single photons. However, recent years have seen successful attempts to build Josephson junction single-photon detectors with advantages of high-speed and low-power operation. In one design, near-infrared single photons can be detected by current-biased JJs as a function of current bias, temperature, photon rate, and polarization [24]. Ultra-broadband Josephson junction single-photon detectors have also been developed using graphene, offering efficient light absorption and very small dark count rates [25].

4. Josephson Junction Detector utilizing waveguide resonators

In this paper, we present a Josephson junction-based detector that utilizes a directional coupler and CPW resonator arrays for detecting signals in both the millimeter and sub-millimeter ranges.

4.1. Theory

We chose to design a structure based on a microstrip λ/2 resonator, as illustrated in figure 6. Instead of using traditional SiO2 as the substrate, we opted for mica over a layer of silicon because mica is suitable for relatively large, molecularly smooth sheets [26].

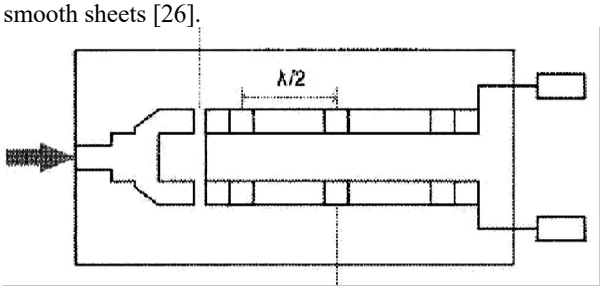

Fig. 6. Schematic of a Josephson junction-based detector using microstrip λ/2 resonator [27].

For our proposed detector, we use a λ/2 resonator on a hybrid substrate, as shown in figure 7. The effective dielectric constant of this substrate can be derived from equation 9.

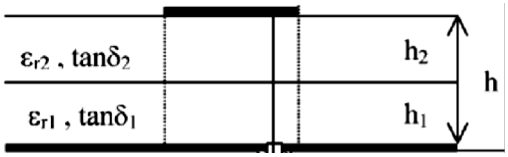

Fig. 7. Schematic of a microstrip resonator with hybrid substrate.

$$\varepsilon_{eff} = \frac{\varepsilon_{r1}\varepsilon_{r2}(h_1+h_2)}{\varepsilon_{r1}h_1+\varepsilon_{r2}h_2} \quad (9)$$

This resonator is part of a periodic Josephson junction lattice, as illustrated in figure 8. We can calculate the quality factor of this structure using equation 10.

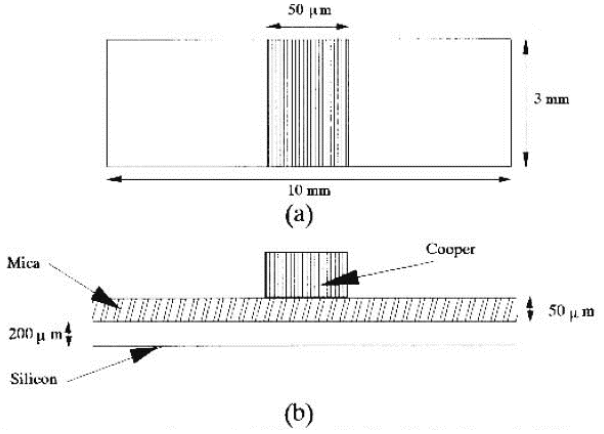

Fig. 8. Structure of a resonator as a part of a periodic Josephson junction lattice (a) from top view and (b) from the side [27].

$$\frac{1}{Q_0} = \frac{1}{Q_n} + \frac{1}{Q_b} + \frac{1}{Q_f} + \frac{1}{Q_d} \quad (10)$$

In this equation, Q_n and Q_b are the quality factors resulting from the losses of the short walls and wide walls of the waveguide, respectively. Q_f and Q_d represent the quality factors resulting from the metal and substrate of the periodic Josephson junction lattice. Furthermore, each of these quality factors is calculated using equation 11.

$$Q_0 = \frac{\omega W}{P_0} \quad (11)$$

Where ω is the frequency of eigen oscillations of the system, W is the EM energy, and P_0 is the power of losses. Mica has a high dielectric constant, so the losses in it are so small that we can overlook them. Therefore, the power of losses in the substrate is dependent on silicon [27].

We used Copper for our millimeter-wave detector and YBCO as the superconductor in our sub-millimeter design. YBCO can exhibit superconductivity at a temperature about 90 K, which is even higher than the boiling point of nitrogen (77 K).

To build an array of detectors, we require a power divider. For this purpose, we selected a short-slot Riblet directional coupler due to its low return loss and high isolation. Riblet couplers are shorter than other coupler designs and are easier to build, which makes them a desirable structure for microwave systems [28]. Furthermore, considering that at the moment, there are no powerful sources available for THz frequencies, balanced mixers with a quadrature coupler can be useful to reduce the required local oscillator (LO) power and the LO sideband noise [29].

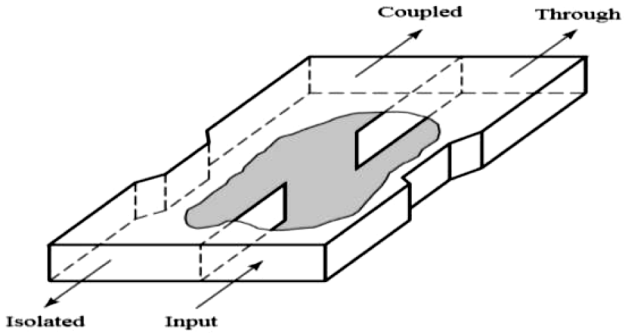

Fig. 9. A Riblet short-slot coupler

4.2. Simulation and results

4.2.1. Millimeter Spectrum Detectors

We designed the resonator shown in Figure 8 using CST for a frequency range between 83 GHz and 100 GHz. This resonator consists of a 0.05 mm wide Cu strip with a thickness of 0.018 mm on a substrate measuring 2.5 mm in width and 10 mm in length. The substrate includes a layer of 0.05 mm thick mica on top of a 0.2 mm thick layer of silicon. The frequency response for this resonator is presented in Figure 11.

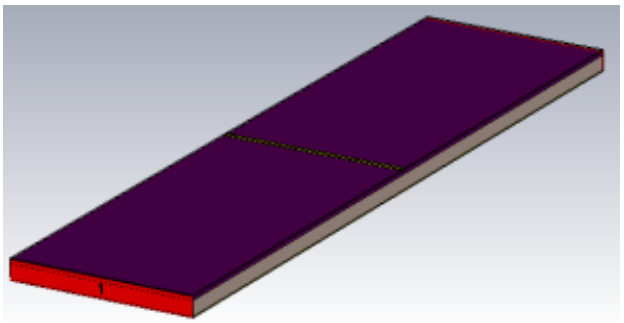

Fig. 10. Schematic of the simulated resonator

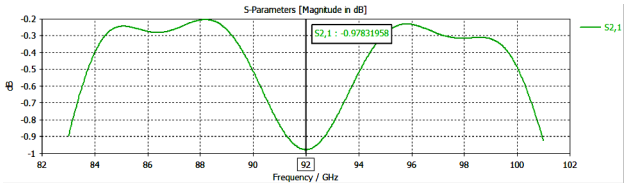

Fig 11. Frequency response for the simulated resonator

For building our array of detectors, we simulated a short-slot hybrid coupler with two-stage linear tapers. This coupler has a simple structure and can be built at a low cost.

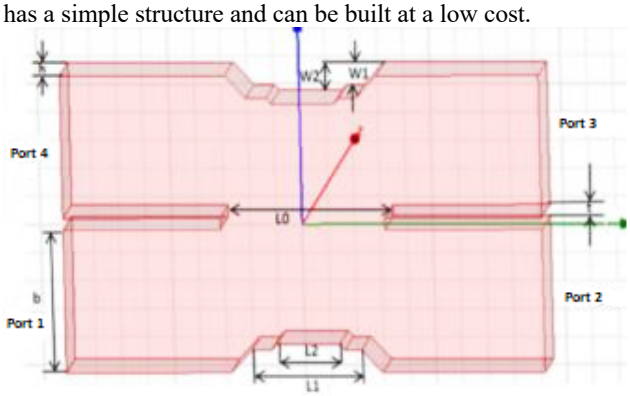

Fig. 12. Schematic of our Riblet short-slot coupler with two tapers

Table 1. The dimensions measurements for our simulated coupler

Dimension	Port width	Port length	Total width	Total length	Gap width	L_0	W_1	L_1	W_2	L_2
Size (mm)	5.22	5.22	2.52	10	0.2	3.4	0.4	2.2	0.5	1.2

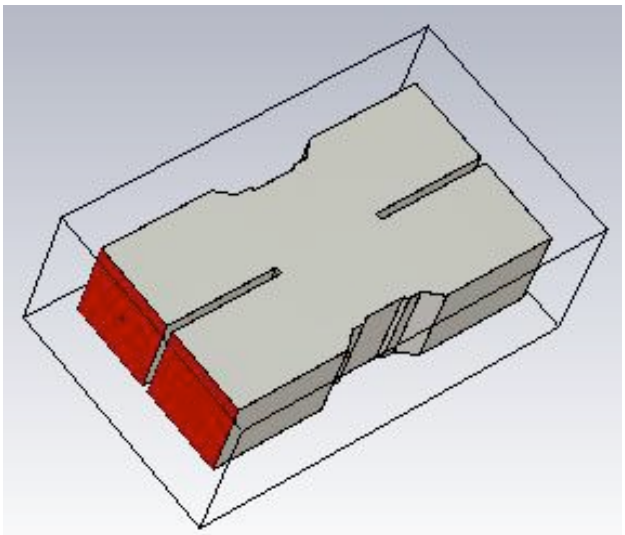

Fig. 13. Riblet short-slot coupler with two tapers simulated in CST

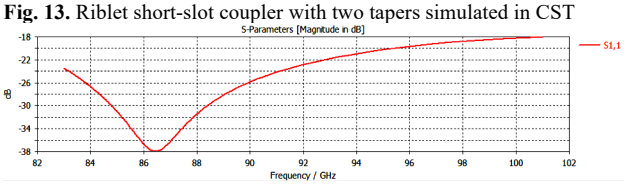

Fig. 14. Return loss of the simulated Riblet short-slot coupler

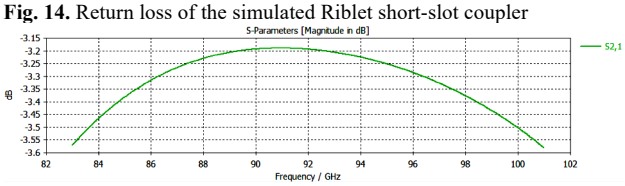

Fig. 15. Output of Port 2 in the simulated Riblet short-slot coupler

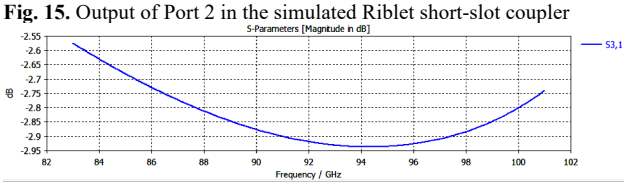

Fig. 16. Output of Port 3 in the simulated Riblet short-slot coupler

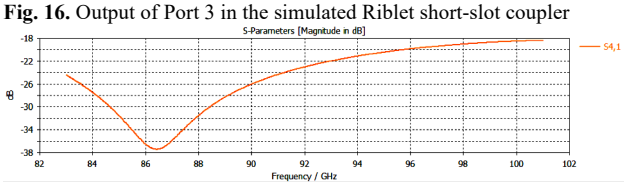

Fig. 17. Isolation of the simulated Riblet short-slot coupler

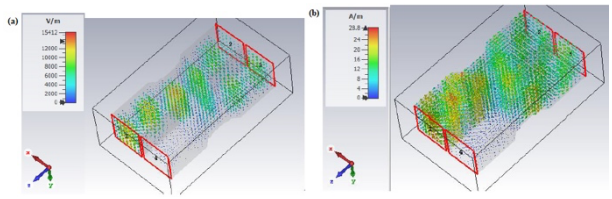

Fig 18. (a) Electric and (b) Magnetic field in the simulated Riblet short-slot coupler

We used this coupler with a 0.1 mm gap between the coupler and the resonator to design a two-resonator array, as shown in Figure 19. This detector showed a loss of 0.215 and a quality factor of 183.011.

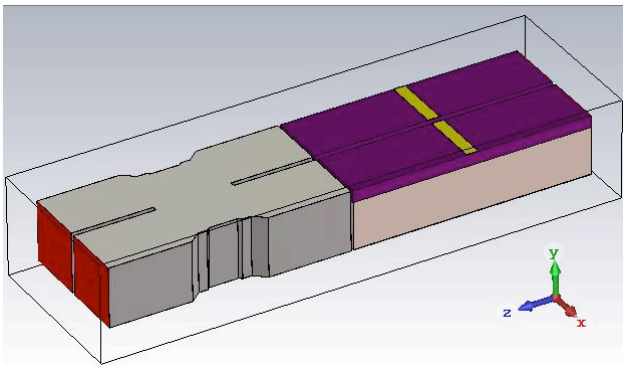

Fig. 19. A two-resonator array

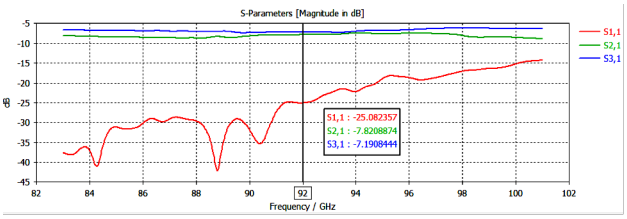

Fig. 20. Frequency response for two-resonator array

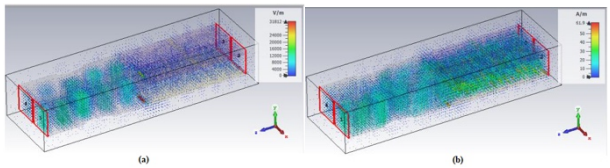

Fig. 21. (a) Electric and (b) Magnetic field in the simulated two-resonator array

We then increased the gap between the coupler and resonator to 0.5 mm and observed that the detector's loss remained almost the same while the quality factor increased to 188.445.We also simulated a four-resonator array with a 0.1 mm gap between the coupler and resonator, as shown in Figure 22. This detector showed a higher loss (0.337) and a higher quality factor (188.577). Similarly, increasing the gap between the coupler and resonator to 0.5 mm led to a higher quality factor (192.321).

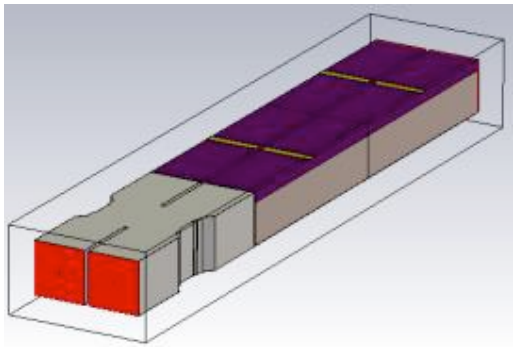

Fig. 22. A four-resonator array

Moreover, we simulated a six-resonator array with a 0.1 mm gap between the coupler and resonator, shown in Figure 23. This time our detector showed a higher loss (0.341) and a higher quality factor (190.577). Similarly, increasing the gap between the coupler and resonator to 0.5 mm led to a higher quality factor (196.517).

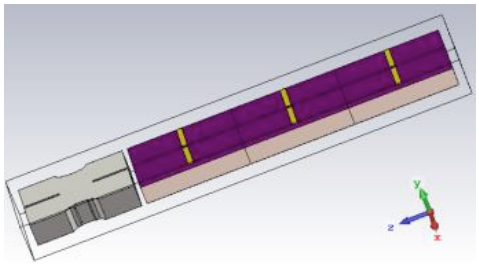

Fig. 23. A six-resonator array

4.2.2. Sub-Millimeter Spectrum Detectors

For a Josephson junction-based detector in the sub-millimeter spectrum, we simulated a resonator in CST for the frequency range between 490 GHz and 510 GHz. This resonator has a similar structure to our millimeter wave detector but with different sizes. It consists of a 0.025 mm wide YCBO strip with a thickness of 0.018 mm on a substrate measuring 0.5 mm in width and 1 mm in length. The substrate includes a layer of 0.2 mm thick mica on top of a 0.2 mm thick layer of silicon. The frequency response for this resonator is presented in Figure 25.

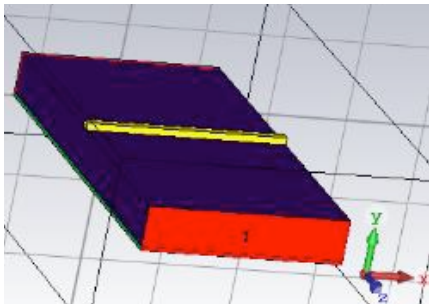

Fig. 24. Schematic of the simulated sub-millimeter resonator

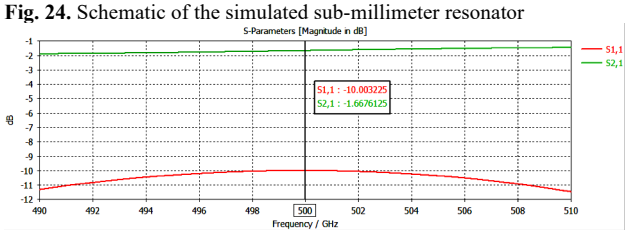

Fig. 25. Frequency response for the simulated resonator

For building our array of detectors, we needed to alter our coupler as well. For this purpose, we simulated a THz-band Narrow-wall 3dB coupler, illustrated in Figure 26, with the sizes shown in Table 2.

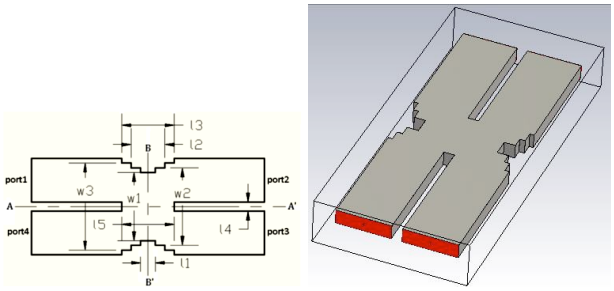

Fig. 26. Schematic of our Riblet short-slot coupler with multiple tapers

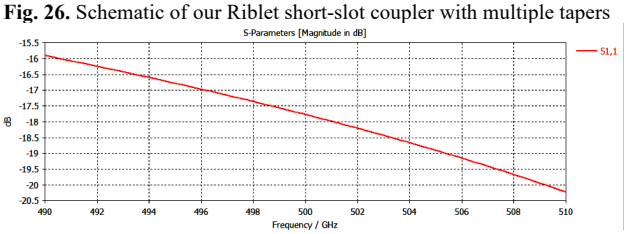

Fig. 27. Return loss of the simulated Riblet coupler

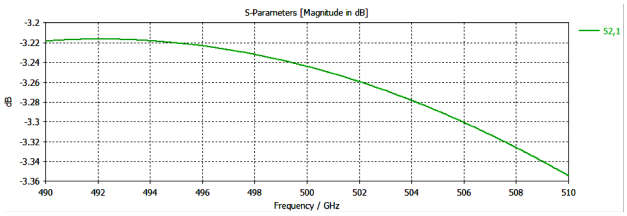

Fig. 28. Output of Port 2 in the simulated Riblet coupler

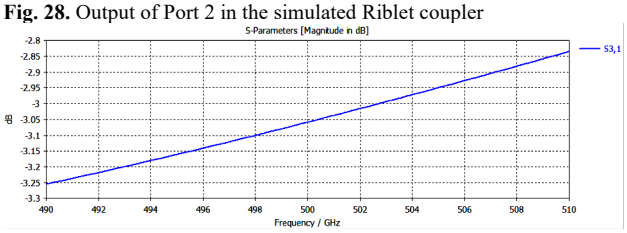

Fig. 29. Output of Port 3 in the simulated Riblet coupler

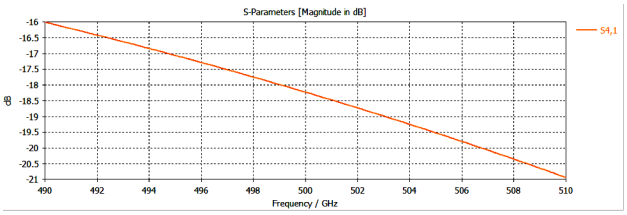

Fig. 30. Isolation of the simulated Riblet coupler

Table 2. The dimensions measurements for our simulated coupler

Dimension	Total width	Total length	Total thickness	L_1	L_2	L_3	L_4	L_5	W_1	W_2	W_3
Size (mm)	1.146	2.969	0.136	0.168	0.376	0.6	0.2	0.6	0.644	0.858	0.962

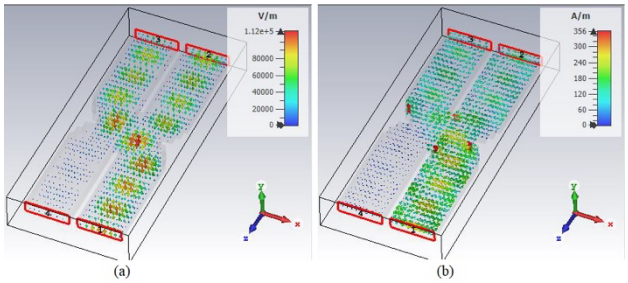

Fig. 31. (a) Electric and (b) Magnetic field in the simulated Riblet coupler

As we did in the millimeter spectrum, we used this coupler to design a two-resonator array, a four-resonator array, and a six-resonator array, once with a 0.1 mm gap between the coupler and resonator and once with a 0.001 mm gap, and compared the results.

We observe that larger arrays provide a higher quality factor; however, the total loss also increases with the number of resonators. Moreover, a smaller gap between the coupler and resonator can result in a higher quality factor but also increase the loss simultaneously. This loss can be attributed to two-level systems (TLS). The disordered structure of amorphous materials causes a two-level system when one or a group of atoms can move from one configuration to another

configuration associated with two local potential energy minima through quantum tunneling over an energy barrier to the other state. TLS causes the electric fields inside a microwave resonator to couple to the dipoles of the TLS, and power will be taken from the resonator and converted to loss, which reduces the quality factor of the resonance. Furthermore, because the random nature of TLS tunneling events causes a random fluctuation in the dielectric constant, it can also result in excess frequency noise in superconducting resonators [30]. So far, no techniques have been proposed to successfully eliminate TLS loss entirely. However, there are ways to reduce losses associated with TLS that require a deeper study of TLS noise, and we did not address it here. Although, it is an interesting subject to explore for further developments in the field of Josephson junction-based detectors.

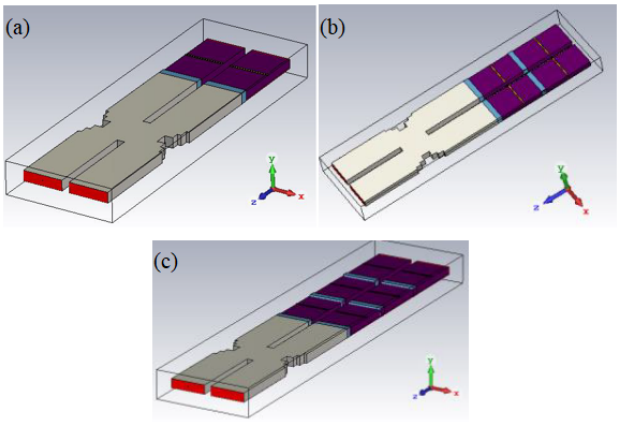

Fig. 32. Schematic of our simulated (a) two-resonator (b) four-resonator (c) six-resonator array

Table 3. Quality factor and loss obtained from each simulation

	two-resonator array	**four-resonator array**	**six-resonator array**
0.1 mm gap	Quality factor= 24663 Loss= 0.173	Quality factor= 25019 Loss= 0.238	Quality factor= 26493 Loss= 0.317
0.001 mm gap	Quality factor= 25320 Loss= 0.306	Quality factor=26453 Loss= 0.427	Quality factor= 29179 Loss= 0.575

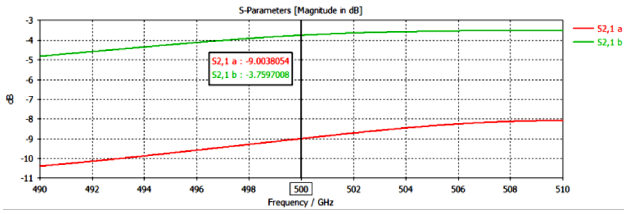

Fig. 33. Frequency response for a two-resonator array with (red) 0.1 mm and (green) 0.001 gap between coupler and resonators

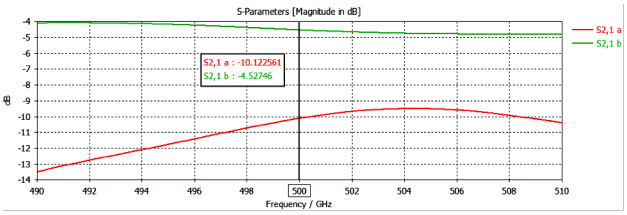

Fig. 34. Frequency response for a four-resonator array with (red) 0.1 mm and (green) 0.001 gap between coupler and resonators

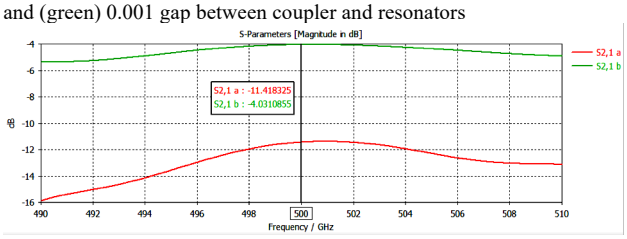

Fig. 35. Frequency response for a six-resonator array with (red) 0.1 mm and (green) 0.001 gap between coupler and resonators

5. Conclusion

Superconducting detectors can provide high sensitivity, broad bandwidth, low noise, and fast response. Detectors using HTS Josephson junctions can be applied to millimeter and sub-millimeter waves and terahertz spectrum with the advantage of small size and low energy. In this paper, we designed and simulated superconducting detectors based on Josephson junction resonators for both millimeter and sub-millimeter waves. For the millimeter spectrum, we simulated a resonator for the frequency range between 83 GHz and 100 GHz and used that resonator in two, four, and six resonator arrays, each time with two different gap lengths between the resonator and coupler. We observed that increasing the gap length had no significant impact on the loss but resulted in an increase in the quality factor. Moreover, both the loss and quality factor increased with the addition of resonators to the array. We repeated this experiment for the sub-millimeter spectrum using a YCBO resonator for the frequency range between 490 GHz and 510 GHz. In this case, we observed that reducing the gap length led to a rise in both loss and quality factor. Furthermore, similar to the millimeter wave simulations, adding resonators to the array led to an increase in both loss and quality factor. The loss in these detectors stems from two-level systems that cannot be fully eliminated; however, it can be managed by adjusting the design, which can be explored in further studies.

References

[1] B. A. Mazin, "Microwave Kinetic Inductance Detectors," California Institute of Technology, Oct. 2005, doi: 10.7907/GZ72-V784.
[2] S. Kumar, "Submillimeter Wave Camera Using a Novel Photon Detector Technology," California Institute of Technology, May 2008, doi: 10.7907/F58T-SV45.
[3] D. P. Kasilingam, "Topics in Millimeter-Wave Imaging Arrays," California Institute of Technology, Mar. 1987, doi: 10.7907/rt21-jt48.
[4] L. Yujiri, M. Shoucri, and P. Moffa, "Passive millimeter-wave imaging," *IEEE Microwave*, vol. 4, no. 3, pp. 39–50, Sep. 2003, doi: 10.1109/MMW.2003.1237476.
[5] O. Noroozian, "Superconducting microwave resonator arrays for submillimeter/far-infrared imaging," California Institute of Technology, Jun. 2012, doi: 10.7907/8MG2-NB23.
[6] G. H. Rieke and L. G. Rubin, "Detection of Light: From the Ultraviolet to the Submillimeter," *Phys. Today*, vol. 48, no. 12, pp. 70–71, Dec. 1995, doi: 10.1063/1.2808304.

[7] J. Zmuidzinas and P. L. Richards, "Superconducting detectors and mixers for millimeter and submillimeter astrophysics," *Proc. IEEE*, vol. 92, no. 10, pp. 1597–1616, Oct. 2004, doi: 10.1109/JPROC.2004.833670.

[8] R. J. Schoelkopf, "Studies of noise in josephson-effect mixers and their potential for submillimeter heterodyne detection," California Institute of Technology, Nov. 1995, doi: 10.7907/xezv-q641.

[9] A. Mourachkine, *High-Temperature Superconductivity in Cuprates*. Dordrecht: Springer Netherlands, 2002. doi: 10.1007/0-306-48063-8.

[10] R. Gross, A. Marx, and F. Deppe, *Applied Superconductivity Josephson Effect and Superconducting Electronics*. Berlin: De Gruyter, 2005.

[11] J. H. Hinken, *Superconductor Electronics Fundamentals and Microwave Applications*. Berlin: Springer-Verlag, Berlin, Heidelberg, 1988.

[12] F. Hegmann, *Picosecond Photoresponse of High-Tc Superconductor Thin Films*. Hamilton: McMaster University, 1994.

[13] J. Sólyom, *Fundamentals of the Physics of Solids*. Berlin, Heidelberg: Springer Berlin Heidelberg, 2007. doi: 10.1007/978-3-540-72600-5.

[14] J. M. Meckbach, *Superconducting Multilayer Technology for Josephson Devices : Technology, Engineering, Physics, Applications*. KIT Scientific Publishing, 2013.

[15] T. Li, J. C. Gallop, L. Hao, and E. J. Romans, "Josephson penetration depth in coplanar junctions based on 2D materials," *J. Appl. Phys.*, vol. 126, no. 17, Art. no. 173901-1-7, 2019, doi: 10.1063/1.5124391.

[16] F. Tafuri, Ed., *Fundamentals and Frontiers of the Josephson Effect*, vol. 286. in Springer Series in Materials Science, vol. 286. Cham: Springer International Publishing, 2019. doi: 10.1007/978-3-030-20726-7.

[17] Du, J., Hellicar, A. D., Li, L., Hanham, S. M., Nikolic, N., Macfarlane, J. C., & Leslie, K. E. (2008). "Terahertz imaging using a high-Tc superconducting Josephson junction detector". *Supercond. Sci. Tech.*, vol. 21, no. 12, pp. 125025–125025*,* Nov. 2008, doi: 10.1088/0953-2048/21/12/125025.

[18] J. Du, "HTS Josephson junction devices for microwave and terahertz applications," *ASEMD 2011*, Sydney, NSW, Australia, 2011, pp. 113-117, doi: 10.1109/ASEMD.2011.6145081.

[19] I. Gundareva, V. Pavlovskiy and Y. Divin, "High-Tc Josephson Junctions as Quasiclassical THz Detectors," *IEEE Trans. Appl. Supercond.*, vol. 28, no. 4, pp. 1-5, Jun. 2018, Art no. 1800105, doi: 10.1109/TASC.2018.2822800.

[20] Y. Divin, U. Poppe, V. N. Gubankov and K. Urban, "High-Tc Josephson Square-Law Detectors and Hilbert Spectroscopy for Security Applications," *IEEE Sens. J.*, vol. 8, no. 6, pp. 750-757, Jun. 2008, doi: 10.1109/JSEN.2008.923185.

[21] E. Holdengreber, A. G. Moshe, M. Mizrahi, V. Khavkin, S. E. Schacham, and E. Farber, "High sensitivity high T_c superconducting Josephson junction antenna for 200 GHz detection," *J. Electromagn. Waves Appl.*, vol. 33, no. 2, pp. 193–203, Oct. 2018, doi: 10.1080/09205071.2018.1535333.

[22] E. Holdengreber, "A Serial Josephson Junction Antenna Array," in *2020 IEEE Int. Conf. Applied Superconduct. Electromagn. Dev. (ASEMD)*, Tianjin, China: IEEE, Oct. 2020, pp. 1–2. doi: 10.1109/ASEMD49065.2020.9276209.

[23] G.-H. Lee *et al.*, "Graphene-based Josephson junction microwave bolometer," *Nature*, vol. 586, no. 7827, pp. 42–46, Oct. 2020, doi: 10.1038/s41586-020-2752-4.

[24] E. D. Walsh, W. Jung, G. H. Lee, D. K. Efetov, B. I. Wu, K. F. Huang, T. A. Ohki, T. Taniguchi, K. Watanabe, P. Kim, D. Englund and K. C. Fong, "Josephson-junction infrared single-photon detector," *Science*, vol. 372, no. 6540, pp. 409–412, Apr. 2021, doi: 10.1126/science.abf5539.

[25] E. Walsh, D. K. Efetov, G. H. Lee, M. Heuck, J. Crossno, T. A. Ohki, P. Kim, D. Englund, and K. C. Fong, "Graphene-Based Josephson-Junction Single-Photon Detector," *Phys. Rev. Appl.,* vol. 8, no. 2, Aug. 2017, doi: 10.1103/physrevapplied.8.024022.

[26] D. Yamamoto, T. Uchihashi, N. Kodera, H. Yamashita, S. Nishikori, T. Ogura, M. Shibata, and T. Ando, "High-Speed Atomic Force Microscopy Techniques for Observing Dynamic Biomolecular Processes," *Methods Enzymol.*, vol. 475, pp. 541–564, Jan. 2010, doi: https://doi.org/10.1016/S0076-6879(10)75020-5.

[27] O. Pustylnik, V. Grmalsky, S. Koshevaya, M. T. Torres, and J. E. Alatorre, "Millimeter waves detector based on Josephson's junctions with optimal substrate," *Int. J. Infrared Milli.,* vol. 287, No. 24, Feb, pp. 1-5, 2006, doi: 10.1007/s10762-006-9069-8.

[28] A. Sarhan, M. Tayarani, H. Oraizi, N. Ghadimi and I. Hamidi, "Optimized broad band riblet short-slot waveguide coupler for X-band applications," *Int. J. Sci. Eng. Res.,* vol. 4, no. 8, pp. 1021-1023, Aug. 2013, ISSN: 2229-5518.

[29] K. Kuroiwa, A. Gonzalez, M. Koyano, T. Kojima, Y. Fujii and Y. Uzawa, "Short-slot Hybrid Coupler Using Linear Taper in W-band," *J. Infrared. Millim. Tech.*, vol. 34, No. 12, pp. 815-823, Dec. 2013. doi: 10.1007/s10762-013-0030-3.

[30] T. Van Duzer, C. W. Turner, and C. W. Turner, *Principles of superconductive devices and circuits*. New York, NY: Elsevier, 1981.